

Mean-field transfer-matrix study of the magnetic phase diagram of CsNiF_3

Y. Trudeau and M. L. Plumer

Centre de Recherche en Physique du Solide, D partement de Physique,
Universit  de Sherbrooke, Sherbrooke, Q bec, J1K 2R1 Canada.

(December 31, 2021)

Abstract

A method for treating ferromagnetic chains coupled with antiferromagnetic interactions on a hexagonal lattice is presented in this paper. The solution of the 1D part of the problem is obtained by classical transfer-matrix while the coupling between the chains is processed by mean-field theory. This method is applied with success to the phase diagram and angular dependence of the critical field of CsNiF_3 . Results concerning the general influence of single-ion anisotropy on the magnetic ordering of such systems are also presented.

I. INTRODUCTION

Mean-field theory has long been a useful approximation for the study of phase transitions in a wide variety of systems, especially magnetic ones.¹ This comes from the great simplification of dealing with an averaged system instead of explicitly taking into account each individual interaction. As is generally the case, the interest here in using mean-field theory is its ability to predict phase transitions and to follow the evolution of relevant quantities close to the transition point. Unfortunately, transition points and critical exponents extracted from the mean-field theory are found to be significantly different from the experimental ones, especially when the effective dimensionality is small. This is due to the averaging process involved which neglects the important critical fluctuations close to the transition point.

Although mean-field theory has some problems when applied directly to low dimensionality systems, it can be a very good approximation if used in conjunction with other techniques. By definition, quasi-one-dimensional (quasi-1D) systems have a direction in which the energy scale is much larger than in the others. Some numerical techniques such as classical transfer-matrix,^{2;3;4;5} quantum transfer-matrix,⁶ and Bethe-Ansatz⁷ can be used to solve almost exactly the 1D part of the problem and so, instead of using mean-field for all the interactions, it can be restricted to the coupling between the chains.⁸ By doing this, important fluctuations, although not the critical ones, will be included and a more accurate solution can be expected.

The present work is mainly concerned with CsNiF_3 and, to some extent other equivalent systems. In this hexagonal insulator, the $S = 1 \text{ Ni}^{2+}$ ions are ferromagnetically coupled in chains, along with the F^- ions. The chains are well separated from each other by large Cs^+ ions and are coupled by antiferromagnetic interactions. This arrangement causes a large spacial anisotropy between the Ni ions, the ratio of the distance between these ions along the chains and in the basal plane being 0.4205, with an interchain separation of 6.27 Å. Anisotropy is thus present in the magnetic properties, the intrachain super-exchange

($J_k = 20 \text{ K}$)⁹ being much larger than the interchain one. The exact ratio between the super-exchange interactions is difficult to estimate because of the strong dipolar interaction arising between the ferromagnetic chains. It is important to note that dipolar field is almost nonexistent if the ordering along the chains is antiferromagnetic (AF), as it is in many other ABX_3 compounds such as CsMnBr_3 and CsNiCl_3 .¹⁰

This strong dipolar field is responsible for the particular planar AF arrangement¹¹ of CsNiF_3 which is different from the expected 120 structure of a system with only AF interactions on a triangular lattice. This magnetic phase occurs for temperatures smaller than $T_N = 2.77 \text{ K}$.¹² Lussier et al.¹² have also shown a strong dependence of the critical field as a function of the angle between the magnetic field and the chain axis. As an example, at $T = 2 \text{ K}$, $H_{c2} = 0.27 \text{ T}$ while for the other direction $H_{c1} = 2.3 \text{ T}$. An unsuccessful attempt was made to fit this peculiar angular dependence of the critical field using a mean-field model similar to the one of Refs. 11 and 13. In this paper, it will be shown that the experimental angular dependence is typical of a system formed by XY ferromagnetic chains with AF coupling between them on a triangular lattice.

The Hamiltonian describing the magnetic properties of such systems is given by:

$$H = \sum_i^X J_k S_i \cdot S_{i+k} + \sum_{\langle a,b \rangle}^X J_a S_a \cdot S_b + g_B H \sum_i^X S_i + D \sum_i^X (S_i)^2 + H_{\text{dipole}} \quad (1)$$

The first, third and fourth sums in equation (1) are along the chain while the second one is between nearest neighbors in the plane perpendicular to the chains axis. The strong XY behavior of CsNiF_3 comes from its large single-ion anisotropy (D) of 8.5 K .⁹ The g -value was set to 2.2.

As mentioned previously, the usual mean-field theory uses averaged quantities for the three lattice dimensions. An example of this is found in Ref. 11. The goal of the present work is to develop a method which treats the chains by classical transfer matrix and uses mean-field for the coupling between them. This method, referred to as MFTM (Mean-Field Transfer-Matrix), is presented in section II. It is followed, in Section III, by a brief review of the transfer-matrix algorithm used to calculate the magnetization and the susceptibility

of a 1D chain as a function of temperature and magnetic field. In Section IV, MFTM is applied to CsNiF_3 for the calculation of its magnetic-field-temperature phase diagram and angular dependence of the critical field. Some other general results, concerning single-ion anisotropy, are presented in Section V.

II. MEAN-FIELD COUPLING OF QUASI-1D CHAINS

Before presenting the calculated phase diagram of CsNiF_3 , it is useful to understand qualitatively the underlying mechanism of the magnetic order in this system. For simplicity, consider a starting point below T_c with a magnetic field oriented in the XY plane, large enough to destroy the AF order. In this phase, the paramagnetic one, the free-energy is dominated by a Zeeman term, $-m \cdot H$, and the magnetization m is parallel to the applied field. As the field amplitude is lowered, this term is diminished up to a point where a perpendicular exchange term, proportional to $J_\perp m^2$, becomes equal to it. At this field, since $J_\parallel < 0$, an AF order develops and a finite angle between the magnetic sub-lattices appears. The critical field, H_c , is defined where this angle is equal to zero. It is important to notice the particular planar structure of the magnetic order in CsNiF_3 (Fig. 1) which is different from the 120 structure of CsMnBr_3 , an XY system having strong AF coupling along the chains. This difference is due to the relatively strong dipolar field originating from the neighboring ferromagnetic chains¹¹. This dipolar field depends strongly on the angle between the magnetic sub-lattices and it can be shown quite easily that there is no interchain dipolar field present on a given site at H_c , where the magnetization of all the sub-lattices are parallel to the field. So, for small angles between the sub-lattices, the order starts to develop like a 120 system (see Fig. 2) but at a given angle, the dipolar field coming from the other chains becomes large enough to flip one of the sub-lattices according to the planar arrangement of CsNiF_3 (Fig. 1).

The starting point of the theoretical description of such a system is the full three-dimensional (3D) Hamiltonian of equation (1). Since this Hamiltonian, applied to a tri-

angular lattice, involves up to three magnetic sub-lattices, it is a highly non-trivial task to solve it even numerically. On the contrary, the one-dimensional (1D) part of the Hamiltonian consisting of first, third and fourth term can be calculated numerically quite easily and with good precision by the transfer-matrix technique. The utility of mean-field theory for this problem comes from the fact that the 1D part has a much larger contribution to the free-energy F than the 3D one ($\langle J_k \rangle \gg \langle J_z \rangle$).⁸ Thermal averages of the 1D Hamiltonian can be used to approximate the free-energy of the 3D one. Formally, this type of free-energy is obtained using the Bogoliubov inequality:¹⁴

$$F - F_T = F_{1D} + \langle H_{1D} \rangle : \quad (2)$$

With the three magnetic sub-lattices of Fig. 2, and with a proper counting of each link in the J_z term, this gives the following trial free-energy:

$$F_T = F_{1D} - \frac{J_z}{g_B H} \sum_i^X (3 \langle S_{ia} \rangle_{1D} \langle S_i \rangle_{1D} + 3 \langle S_{ia} \rangle_{1D} \langle S_i \rangle_{1D} + 3 \langle S_{ib} \rangle_{1D} \langle S_i \rangle_{1D} + 3 \langle S_{ic} \rangle_{1D} \langle S_i \rangle_{1D}) \\ + \sum_i^X (H \langle S_{ia} \rangle_{1D} + H \langle S_{ib} \rangle_{1D} + H \langle S_{ic} \rangle_{1D}) \quad (3)$$

The thermal averages $\langle S_{ia} \rangle$ are just the magnetisation m of the sublattice a . Using the angle definition of Fig. 2 for θ and defining ϕ as the angle between the field and the XY plane, the trial free-energy can be written as:

$$F_T = F_{1D} - 3J_z (2 \cos \theta + \cos 2\theta) m^2 \\ (1 + 2 \cos \phi) \cos \theta m_\phi ; \quad (4)$$

where m_ϕ is the component of m in the XY plane.

It is also important to note that equation (4) is valid only for small values of the angle θ where the dipolar field has no influence on the order. Minimising (4) with respect to θ gives $\sin \theta = 0$ or,

$$\cos \theta = \frac{1}{2} \frac{\cos \phi}{\cos \theta} + \frac{J_z}{J_z} : \quad (5)$$

This result is reasonable. At high fields, $\theta = 0$, indicating the field-induced ferromagnetic (paramagnetic) phase. In zero field, and for a sufficiently low temperature, one gets

the 120° configuration. Of course, this type of structure is not applicable for CsNiF_3 but it reflects the ordering mechanism which is valid only for small values of β . As indicated above, H_c is defined where $\cos \beta = 1$ and it can be obtained by solving self-consistently the following equation:

$$3J_2 m^2 = \cos \beta H m \quad (6)$$

Each side of equation (6) represents a contribution to the free-energy F (to within a minus sign). The right-hand side is the magnetic field contribution $-m H$, the dominant one in the paramagnetic phase, while the left-hand is the 3D contribution of the ordered phase. Since m is bounded to unity, the field contribution will eventually dominate at high field and the phase with the lowest free-energy will be the paramagnetic one. The strength of the ordered phase is controlled by the parameter J_2 . In some systems, like CsNiF_3 , this parameter is not well known but it can be evaluated with this technique by fitting to experimental data.

From the limiting behavior of equation (6) at low field, it is also possible to calculate, within MFTM, the transition temperature in zero field⁸, T_c . This gives:

$$\chi_{1D}(T_c; 0) = \frac{1}{3J_2} \quad (7)$$

where χ_{1D} is the 1D susceptibility. An interesting application of equation (7) is the possibility to calculate directly the value of J_2 needed for a given T_c . In the present work, this is the only procedure used to set J_2 .

The last item that needs to be solved in this mean-field theory is the value and the orientation of the external magnetic field H_{ext} . Up to now, the field included in the calculation was the effective field applied to 1D chain. This is not the true external field; one needs to add a dipolar contribution H_{dip} and a 3D contribution, H_{3D} , coming from the influence of the neighboring chains. Using H_{1D} to designate the field used previously in this paper this gives:

$$H_{\text{ext}} = H_{1D} + H_{3D} + H_{\text{dip}} \quad (8)$$

Equation (8) is shown graphically in Fig. 3. This figure also shows two new angle definitions between fields and the X-Y plane: θ_{ext} for H_{ext} and θ_m for H_{3D} and H_{dip} . The evaluation of H_{3D} is straightforward it is just the number of near neighbors times J_z . It gives:

$$H_{3D} = 6J_z m \quad (9)$$

The dipolar field H_{dip} can be evaluated easily, if the magnetization of all the sub-lattices are parallel, since there is no interchain contribution. For m in the plane perpendicular to the chain this gives:

$$H_{\text{dip}} = \frac{32}{3} K m \quad ; \quad (10)$$

with

$$K = \frac{g^2 \mu_B^2}{4 a^3 k_B} : \quad (11)$$

Since CsNiF_3 has a quite strong X-Y character, the component of m in the X-Y plane was always by far the greatest for all the angles used in the calculation so that the numerical constant used in equation (10) was good to a few percent in all cases.

The fields H_{3D} and H_{dip} are important in evaluating the external field H_{ext} but they are not included in the calculation of H_c by equation (6). The first one, H_{3D} , is implicitly accounted for in the left-hand side of equation (6) while the second one, H_{dip} , obviously turns with m so there is no free-energy changes due to it.

The phase transitions are obtained by the solution of equation (6) which implies a prior knowledge of $m(T; H)$, the 1D magnetization. An effective and flexible way of calculating m is the transfer-matrix technique, which depends on the various 1D parameters like the single-ion anisotropy (D) and the parallel exchange interaction (J_k).

III. TRANSFER-MATRIX TECHNIQUE

Since the present work relies heavily on the transfer-matrix technique, a brief summary of this method is presented here. This study follows the work of Blume et al.² and assumes that the classical spin Hamiltonian for an N spins chain of magnitude S can be written as:

$$H_s = \sum_{i=1}^N V(\hat{S}_i; \hat{S}_{i+1}); \quad (12)$$

with

$$V(\hat{S}_i; \hat{S}_{i+1}) = J \hat{S}_i \cdot \hat{S}_{i+1} - \frac{D}{2} [(\hat{S}_i^z)^2 + (\hat{S}_{i+1}^z)^2] + \frac{H}{2} (\hat{S}_i + \hat{S}_{i+1}) \quad (13)$$

and

$$J = \frac{J_k S(S+1)}{j_k S(S+1)} \quad \begin{matrix} n \\ J = 1 \end{matrix} \quad \begin{matrix} F \\ J = 1 \end{matrix} \quad \text{AF} \quad (14)$$

$$D = \frac{D S(S+1)}{j_k S(S+1)} \quad \begin{matrix} n \\ D < 0 \end{matrix} \quad \begin{matrix} \text{Ising} \\ D > 0 \end{matrix} \quad \text{XY} \quad (15)$$

$$H = \frac{g_B H \sum_{i=1}^N S(S+1)}{j_k S(S+1)} \quad (16)$$

$$\sim = j_k S(S+1) \quad (17)$$

The unit vectors \hat{S}_i are oriented along the spin direction. Using these definitions, the partition function can be written¹⁴ as a product of Boltzmann factors,

$$\begin{aligned} Z &= \sum_{\{S_i\}} \exp \left[- \sum_{i=1}^N V(\hat{S}_i; \hat{S}_{i+1}) \right] \\ &= \sum_{\{S_i\}} \prod_{i=1}^N \exp \left[- V(\hat{S}_i; \hat{S}_{i+1}) \right] : \end{aligned}$$

Since V is translationally invariant, the term in the product does not depend on the site chosen and Z is given by:

$$Z = \text{Tr} K^N \quad (18)$$

with

$$K = \sum_{i=1}^N \exp \left[- V(\hat{S}_i; \hat{S}_{i+1}) \right] \quad (19)$$

Since N is a very large number, only the largest eigenvalue λ_0 of K will contribute significantly to Z .

For classical spins, the transfer-operator K needs to be mapped onto some discretisation of the spherical coordinates in order to evaluate it numerically. Following the procedure found in Ref. 5, which is suitable for broken rotational symmetry, one finds the 1D magnetization to be given by:

$$m = \sum_{i=1}^N \sum_{j=1}^N W_i W_j \mathbf{e}_0(\mathbf{i}; \mathbf{j}) \mathbf{e}_0(\mathbf{i}; \mathbf{j}) [\cos(\theta_i) \hat{z} + \sin(\theta_i) \cos(\phi_j) \hat{x} + \sin(\theta_i) \sin(\phi_j) \hat{y}]; \quad (20)$$

where \mathbf{e}_0 is the eigenvector of K corresponding to the largest eigenvalue λ_0 and, $N_\theta, N_\phi, W_\theta, W_\phi$, are respectively the number of coordinates and the Legendre weights of the discretised spherical coordinates θ_i and ϕ_i . In the absence of a magnetic field, or when the field is along the chain axis, a simplification using the rotational invariance of V can be used.⁴ The reduced number of coordinates for K greatly improves the amount of computing time needed for a given precision. Such a simplification can be used to evaluate the susceptibility of the zero field equation (7). Using the results found in Ref. 2 the 1D susceptibility can be written as:

$$\begin{aligned} \chi_{1D}^{zz}(q) &= \frac{1}{2} \sum_{i=1}^N \frac{\lambda_{00}^2 \lambda_{10}^2}{\lambda_{00}^2 \lambda_{10}^2 \cos q + \lambda_{10}^2} \sum_{i=1}^N W_i \cos(\theta_i) \lambda_{00}(\theta_i) \lambda_{10}(\theta_i) \\ \chi_{1D}^{xx}(q) &= \frac{1}{2} \sum_{i=1}^N \frac{\lambda_{00}^2 \lambda_{11}^2}{\lambda_{00}^2 \lambda_{11}^2 \cos q + \lambda_{11}^2} \sum_{i=1}^N W_i \cos(\theta_i) \lambda_{00}(\theta_i) \lambda_{11}(\theta_i) : \end{aligned} \quad (21)$$

When using the rotational invariance as a simplification, one needs to introduce a second index in order to specify the azimuthal dependence. This second index is implicitly taken into account with the broken rotational symmetry algorithm. Typical matrix sizes are $28^2 \times 28^2$ for the broken rotational symmetry algorithm while they are only 64×64 for the rotational invariance one. In both cases the amount of computing is not excessive, ranging between seconds and minutes per $(T; H)$ point. Of course this figure increases rapidly with matrix size.

IV. APPLICATION TO CsNiF_3

The main goal of this work is to calculate the magnetic phase diagram of CsNiF_3 . Figure 4 presents a comparison between the experimental phase diagram obtained with ultrasound

by Lussier et al.¹² and the phase diagram calculated with the MFTM method. In this figure, the circles are the original experimental data and the squares are from the MFTM. The diamond at zero field is set to 2.77 K by an appropriate choice of J_z according to equation (7). The value found for J_z using this procedure is 0.0253 K. For this phase diagram and all the subsequent MFTM data on CsNiF_3 it will be the only value of J_z used. The overall agreement between theory and experiment is good considering the fact that this mean-field theory neglects the 3D fluctuations which are not included in the transfer-matrix calculation and are the relevant ones close to T_c . It is quite obvious from the development of MFTM that H_c scaled as m and so $H_c \propto (T_N - T)$. The absence of the 3D fluctuations thus reflects itself in the critical exponent, giving the usual mean-field value of $1/2$ value for the theoretical phase diagram. This compares with an experimental estimate¹² of $\beta = 0.31$.

The large XY single-ion anisotropy in CsNiF_3 has an important effect on the angular dependence of H_c . Crudely, one can say that when increasing the field for $T \rightarrow T_c$ the transition occurs when m saturates so that the left side of equation (6) becomes bounded and the H term at the right can dominate. Because of the XY anisotropy of CsNiF_3 , m will grow rapidly along the projection of H in the XY plane and it will saturate for approximately the same field for small angles of the field out of the plane. For large angles, the projection of H in the XY plane will be small and m will grow more slowly giving a larger H_c . This type angular dependence is shown in Fig. 5. In this figure, the experimental data of Ref. 12 and the MFTM results are represented respectively by the circles and the diamond. The agreement, already quite good between these data, becomes excellent when a possible correction for a misalignment of the experimental plane of rotation of 6° is included (circles). This correction, although large, is not unreasonable. One should also consider the nature of the theoretical method used as a source of error, especially close to $\theta = 90^\circ$, a pathological angle for the present method since the coupling between m_z and H then tends to zero. As mentioned earlier, even for the largest angle of the magnetic field out of the XY plane used, m was always out the plane by less than 10° so that the numerical constant in equation (10) was valid to a few percent. The good agreement found in Fig. 5 constrains

sharply with the failure of full 3D mean-field theory, as mentioned in Ref. 12.

V. SINGLE-ION ANISOTROPY

More generally, in the absence of a magnetic field, the paramagnetic phase transitions are determined by the magnetic susceptibility of the system according to equation (7). When a single-ion anisotropy is present, like in the Ising and XY cases, the susceptibility is not isotropic and only the largest component needs to be taken into account. For an Ising system it is the longitudinal component $\chi_{1D}^{zz}(0)$ while for an XY one, it is one of the transverse components $\chi_{1D}^{xx}(0)$ or $\chi_{1D}^{yy}(0)$. The equation (7) is particularly useful since from the knowledge of the susceptibility at a given temperature one can extract the perpendicular exchange interaction J_{\perp} needed for a phase transition at this temperature. Such plots, for various values of D in a system having $J_k = 1$ and $S = 1$ are shown in Fig. 6. One can observe in this figure three limiting cases; the Heisenberg one at high values of J_{\perp} , the XY one at intermediate values and the Ising one at low values. This can be easily understood, the general effect of the single-ion anisotropy is to favor the order by increasing the susceptibility when reducing the degrees of freedom of the spin system. It is especially true if the anisotropy is of the Ising type since the degrees of freedom become discrete. The XY anisotropy has a similar influence but it is less pronounced, the degrees of freedom being still continuous. Of course, at high enough temperature ($T \gg D = k_B$) the Heisenberg behavior is recovered in all cases.

There is a functional difference between the continuous and discrete degrees of freedom. For the continuous ones, the low J_{\perp} behavior is characterised by a power law of the form $T_c \propto J_{\perp}^{1/2}$. The dotted line, having a 1/2 slope, helps appreciate this. On the contrary, the discrete one (Ising) shows a more complex exponential form. These results are in agreement with the arguments of Villain et al.¹⁵ Their result for the Ising case is shown by the dashed curve.

The last aspect investigated in this paper is the influence of the amplitude of the XY

single-ion anisotropy on the whole phase diagram. As seen in the previous paragraph an increase of the anisotropy will enhance the magnetic order as a function of the temperature by increasing the susceptibility. As a function of the magnetic field, for $T > T_c$, the anisotropy should have a much smaller effect since it is not implied directly in the phase transition. Figure 7 shows such phase diagrams for a magnetic field in the $X-Y$ plane and for three values of \tilde{D} ; 0.1, 0.2 and 0.5. The value of J_z has been set arbitrarily and the same lattice parameters than CsNiF_3 have been used. In zero field, the predicted behavior is observed, the highest T_c being with $\tilde{D} = 0.5$ while the lowest is with $\tilde{D} = 0.1$. For a constant temperature smaller than T_c (like $T=2J_k = 0.06$), one can also observe the small effect of \tilde{D} on H_c .

V I. C O N C L U S I O N

In this work, a method for treating antiferromagnetically coupled ferromagnetic chains by mean-field theory has been developed for a system with a hexagonal lattice. The solution of the 1D part of the problem has been obtained by a generalised transfer-matrix algorithm which is suitable for broken rotational symmetry.⁵ Although special care has been needed to correctly account for the large dipolar field originating from the ferromagnetic chains, it has been possible to reproduce with success the phase diagram of CsNiF_3 by only adjusting the value of J_z . The peculiar dependence of the critical field of CsNiF_3 as a function of the angle between the magnetic field and the chain axis has also been reproduced successfully,¹² in sharp contrast with 3D mean-field theory.

More generally, the dependence of the critical temperature as a function of J_z has been established for various values of the single-ion anisotropy D . For the cases having continuous degrees of freedom, like the $X-Y$ and Heisenberg ones, a $T_c \propto J_z^{1/2}$ has been found while for the Ising case a more complex form has been obtained. These results are all in agreement with the ones obtained by Villain et al in Ref. 15. For the $X-Y$ case, the effect of the size of the single-ion anisotropy on the overall shape of the phase diagram have also been investigated.

The results are in agreement with some simple physical arguments, an increase of T_c with D and a rather small effect on H_c for temperatures much lower than T_c .

On the basis of the success of this method for the phase diagram of CsNiF_3 , some extensions can be considered. The phase diagram of AF-chains compounds with XY behavior, like CsMnBr_3 ,¹⁰ could be examined although some complications with the transfer-matrix algorithm, coming from the difference in the effective field of the two staggered sub-lattices, are expected. Since successive phase transitions occur, the present method, based on linear response theory, must be generalized so that the free-energy itself is calculated.¹⁶ A more challenging prospect is the application of this method to easy-axis AF chains systems like CsNiCl_3 .¹⁰ In this case, the single-ion anisotropy plays an active role in the magnetic ordering so it cannot be taken into account only by the transfer-matrix solution of the 1D part of the problem; it must also be included in the calculation 3D free-energy. This will add at least an order of magnitude to the complexity of the problem.

ACKNOWLEDGMENTS

Financial support from the Centre de Recherche en Physique du Solide, the Natural Sciences and Engineering Research Council of Canada and le Fonds Formation de Chercheurs et l'Aide à la Recherche du Gouvernement du Québec has been essential for this work. We also want to thank B. Lussier for his experimental data.

REFERENCES

- ¹ H . Eugene Stanley, Introduction to phase transitions and critical phenomena, Oxford Science Publication, 79 (1971).
- ² M . Blum e, P . Heller and, N . A . Lurie, Phys. Rev. B 11, 4483 (1975).
- ³ J. M . Loveluck, J. Phys. C , 12, 4251 (1979).
- ⁴ J.-G . Dem ers and A . Caille, Solid State Com m . 68, 859 (1988).
- ⁵ Y . Trudeau, A . Caille, M . Poirier, and J.-G . Dem ers Solid State Com m . 82, 825 (1992).
- ⁶ T . Delica and H . Leschke, Physica A 168, 736 (1990); T . Delica, W . J. M . de Jonge, K . Kopinga, H . Leschke and H . J. M ikeska, Phys. Rev. B 44, 11 773 (1991).
- ⁷ M . Takahashi: Phys. Rev. B 43 5788, (1991).
- ⁸ D . J. Scalapino, Y . Im ry and P . P incus, Phys. Rev. B 11, 2042 (1975).
- ⁹ C . Dupas and J. P . Renard, J. Phys. C 10, 5057 (1977).
- ¹⁰ M agnetic System s w ith C om peting Interactions, edited by H . T . D iap, W orld Scientific, Singapour, (1994).
- ¹¹ M . Scherer and Y . Barjoux, Phys. Status Solidi B 80, 313 (1977). N . Suzuki, J. Phys. Soc. Jpn. 52 3199 (1983) M . L . Plumer and A . Caille, Phys. Rev. B 37, 7712 (1988).
- ¹² B . Lussier and M . Poirier, Phys. Rev. B 48,
- ¹³ M . Poirier, M . Castonguay, A . Caille, M . L . Plumer and B . D . Gaulin, Physica B 165-166, 171 (1990).
- ¹⁴ J. J. Binney, N . J. D owrick, A . J. Fisher, and M . E . J. Newman, The theory of critical phenomena, Oxford Science Publications, 61 (1992).
- ¹⁵ J. Villain and J. M . Loveluck, J. Phys. 38, L-77 (1977).

¹⁶O .Heinonen, Phys. Rev. B 47, 2661, (1993).

FIGURES

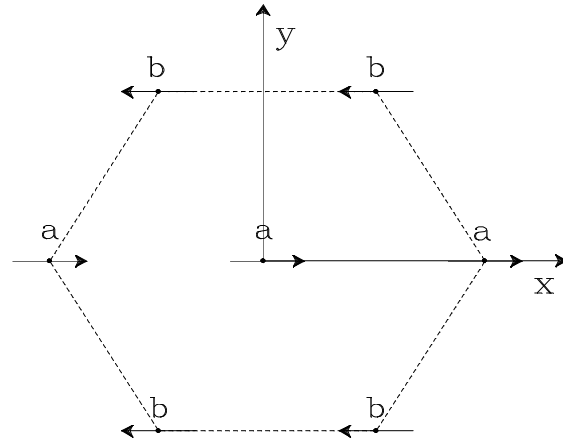


FIG .1. Planar arrangement of the two magnetic sub-lattices of CsNiF_3 for $H = 0$ and $T < T_c$.

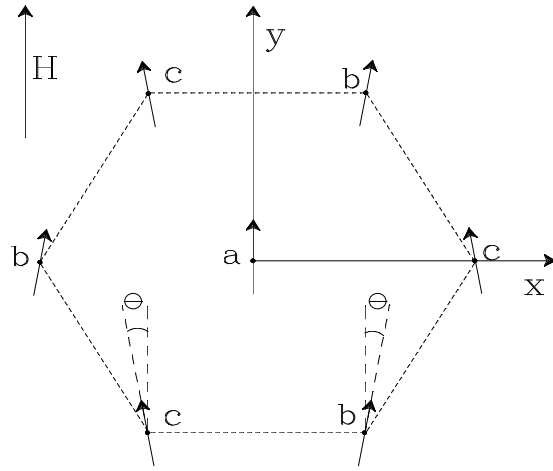


FIG .2. Ordering of a three antiferromagnetic sub-lattice system at a magnetic field close to H_c .

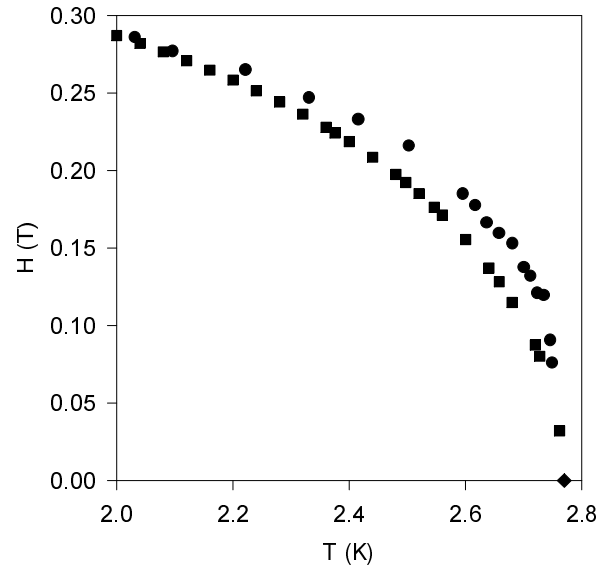
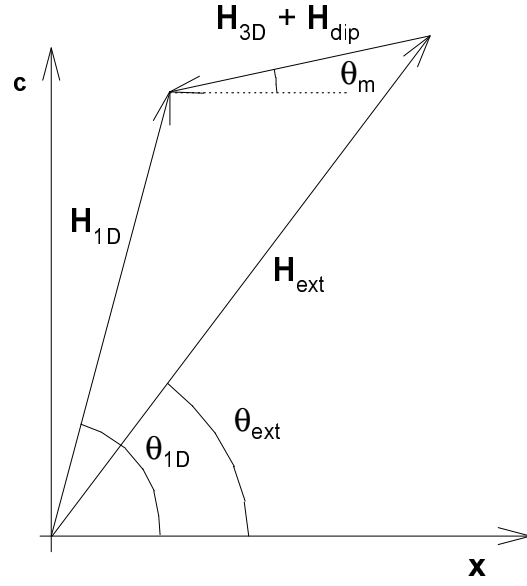


FIG. 4. Comparison between the experimental phase diagram of $CsNiF_3$ given in Ref. 12 (circles) and the one calculated by the method described in this paper (squares). The diamond represent the zero field point used to set J_2 according to eqn. (7).

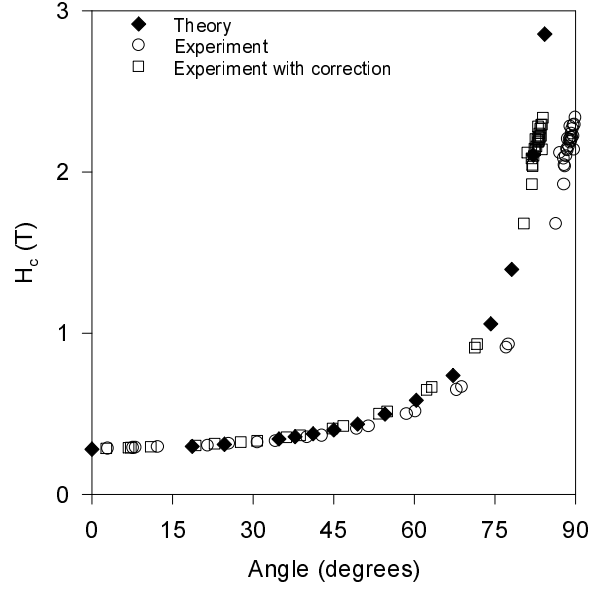


FIG. 5. Comparison between the experimental angular dependence of H_c at $T = 2$ K given in Ref. 12 (circles and squares) and the one calculated by the method described in this paper (diamond). The squares represent the original data (circles) corrected for a plane of rotation misalignment of 6° .

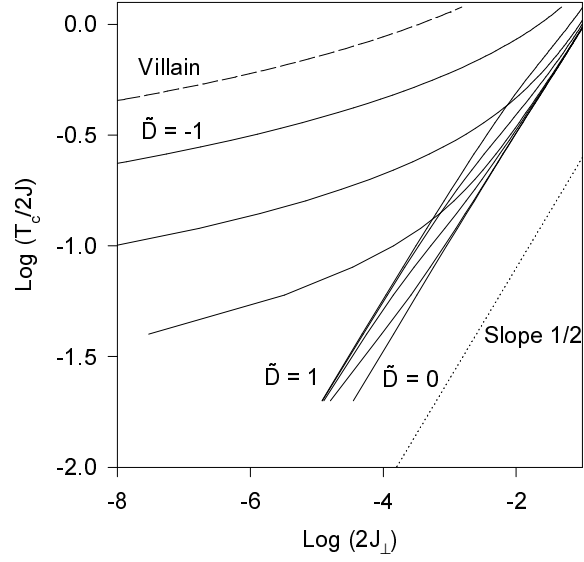


FIG . 6. Logarithm of the critical temperature T_c versus $2J_{\perp}$ for various \tilde{D} values. The curves are for $\tilde{D} = 0, 0.001, 0.01, 0.1, 1, -0.1$.

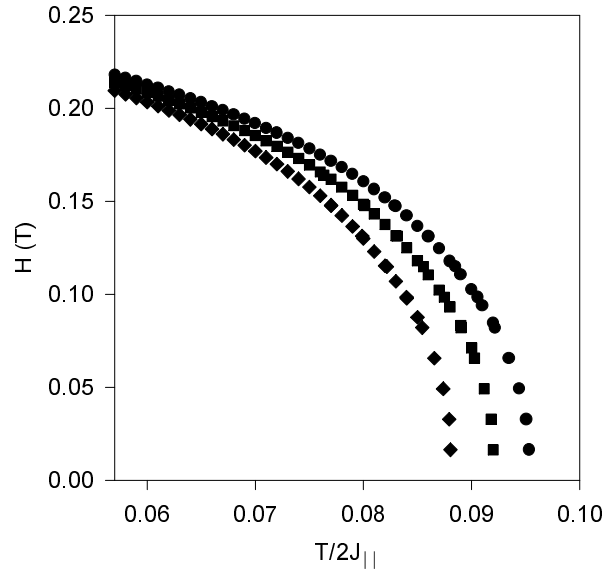


FIG . 7. Magnetic phase diagrams for various D values; 0.5 (circles), 0.2 (squares) and 0.1 (diamond). The J_z has been set arbitrarily.